Chapter 4

Double-scale Pulses Generated by Mode-locked Fibre Lasers and Their Applications

Sergey Kobtsev, Sergey Smirnov and Sergey Kukarin

Additional information is available at the end of the chapter

http://dx.doi.org/10.5772/61956

Abstract

This chapter presents a detailed analysis of properties of double-scale pulses (also called noise-like pulses and femtosecond clusters) generated in fibre lasers and gives an in-depth discussion of promising applications of such pulses.

Keywords: Fibre laser, passive mode locking, ultrashort pulse, non-linear polarisation evolution, double-scale pulse, noise-like pulse, laser radiation, mode correlations

1. Introduction

Mode-locked fibre lasers possess an intriguing capability of emitting, in certain generation regimes, a regular train of pico- or nanosecond wave packets stochastically filled with femtosecond sub-pulses. In the available literature on the subject, these wave packets are referred to as noise-like pulses [1–3], noise bursts [4], double-scale lumps [5], femtosecond clusters [6] or double-scale pulses [7]. In the scope of this chapter, we use the latter of these terms while discussing properties and applications of such pulses.

Until recently, double-scale pulse generation was only achieved in mode-locked fibre lasers, and there is still no understanding of physical mechanisms leading to formation of double-scale pulses, *i.e.,* to the co-existence of a virtually stable envelope of wave packets with power and phase fluctuations inside the wave packets. Parameters of these ultrashort pulses (such as peak power, duration, energy or instantaneous frequency) may experience significant fluctuations both during a single double-scale pulse and from one such pulse to another. Coherence time of double-scale pulses is determined by the duration of sub-pulses, which latter may be substantially shorter than that of the wave packet as a whole. As a result, such pulses have two different typical duration scales. The shape of the intensity autocorrelation

function (ACF) is a characteristic 'fingerprint' of double-scale pulses with its very distinct narrow central peak sitting on top of a broad pedestal. The width of this narrow peak corresponds to the typical sub-pulse duration and usually amounts to several hundred femtoseconds.

Double-scale pulses were mentioned for the first time at the close of the 1990s [1], when pulses with broad spectrum and noise-like behaviour of their intensity and phase were generated in a mode-locked erbium laser. For a long time, double-scale pulses were disregarded as 'not sufficiently coherent', and thus did not draw substantial attention to the respective laser generation regimes. Nevertheless, over recent years, this topic has been rapidly gaining popularity after the observation of double-scale pulses with relatively high energy in ultralong fibre lasers. Active research prompted by this discovery has shown that double-scale pulses may even be preferable in a number of applications, including non-linear frequency conversion, such as harmonic generation [8], Raman conversion [9] or super-continuum generation [10–13], as well as applications in imaging and sensing systems with high temporal and/or spatial resolution. It was furthermore demonstrated that generation of double-scale pulses in long lasers represents a remarkably multiform phenomenon encompassing many non-linear optical mechanisms, whose interaction may result in the emergence of diverse spatio-temporal coherent structures in laser radiation [14].

Here, we present a detailed analysis of double-scale pulse properties and provide an in-depth discussion of the above-mentioned and other important and promising applications of double-scale pulses generated in mode-locked fibre lasers.

2. Generation of double-scale pulses

The most common way to generate double-scale pulses is *via* fibre lasers passively locked due to the effect of non-linear polarisation evolution (NPE). It should also be noted that to date double-scale pulses have been demonstrated in other types of passively mode-locked lasers, including those using saturable absorbers made of single-walled carbon nanotubes [15], as well as topological insulators [16] and non-linear loop mirrors or amplifiers (NOLM/NALM) [11, 17, 18]. Nonetheless, NPE lasers possess the largest number of degrees of freedom in adjustment of the generation regime. This greatly facilitates realisation of various generation regimes in them, including double-scale generation ones [5, 7, 14].

A typical configuration of a fibre laser passively mode-locked due to NPE is presented in Fig. 1. In most reported research, laser-diode-pumped (LD) erbium- or ytterbium-doped optical fibres are used as the active medium. Since their generation spectrum is rather wide, NPE-mode-locked lasers are most often implemented in ring-cavity configuration, thus avoiding the need for broadband reflectors. Optical isolators are normally used to ensure unidirectional generation. Adjustment and switching of generation regimes are done with intra-cavity polarisation controllers PC1 and PC2. The generated laser radiation can be extracted from the cavity either through fibre couplers or through one of the ports of the fibre-optical polarisation

http://dx.doi.org/10.5772/61956

beam splitter, which also carries the function of introducing polarisation-dependent optical losses, thus ensuring passive NPE mode locking.

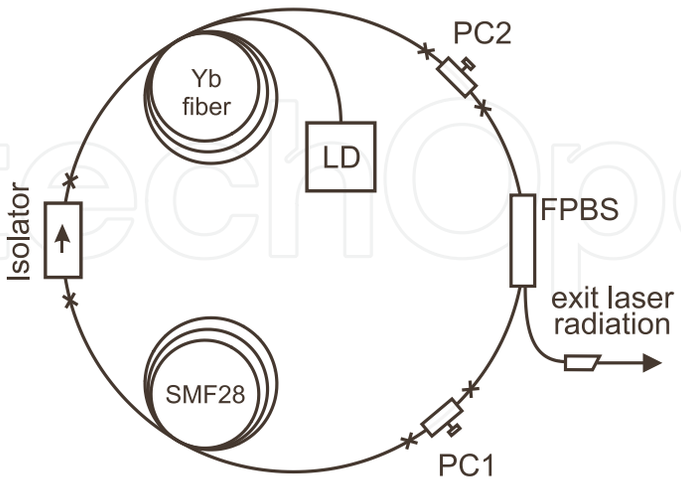

Figure 1. Typical layout of a fibre laser passively mode-locked due to the NPE effect.

In relatively short lasers (with few-meter-long cavities), both double-scale and 'usual' pulses (as well as some transitional or intermediate regimes between these two) may be generated at different settings of the intra-cavity polarisation controllers or the pump power level (see Fig. 2). In contrast, elongation of the fibre laser cavity to several hundred metres or several kilometres leads to predominant generation of double-scale pulses [19, 20]. Cavity elongation is one of the most effective ways to raise the output pulse energy in passively mode-locked lasers [21]; therefore, double-scale pulses became the focal point of research conducted by many groups around the world. Various publications studied spectral and temporal properties of double-scale pulses produced in different generation regimes [22–25].

3. Direct numerical simulation of double-scale pulses

Numerical modelling of double-scale pulse generation in fibre lasers is usually based on the generalised non-linear Schrödinger equation (GNLSE) [20] or on a system of simultaneous equations for polarisation components of the intra-cavity radiation [5]:

$$\frac{\partial A_x}{\partial z} = i\gamma\left\{\left|A_x\right|^2 A_x + \frac{2}{3}\left|A_y\right|^2 A_x + \frac{1}{3}A_y{}^2 A_x^*\right\} + \frac{g_0/2}{1+E/\left(P_{sat}\cdot\tau\right)}A_x - \frac{i}{2}\beta_2\frac{\partial^2 A_x}{\partial t^2} \quad (1)$$

$$\frac{\partial A_y}{\partial z} = i\gamma\left\{\left|A_y\right|^2 A_y + \frac{2}{3}\left|A_x\right|^2 A_y + \frac{1}{3}A_x{}^2 A_y^*\right\} + \frac{g_0/2}{1+E/\left(P_{sat}\cdot\tau\right)}A_y - \frac{i}{2}\beta_2\frac{\partial^2 A_y}{\partial t^2} \quad (2)$$

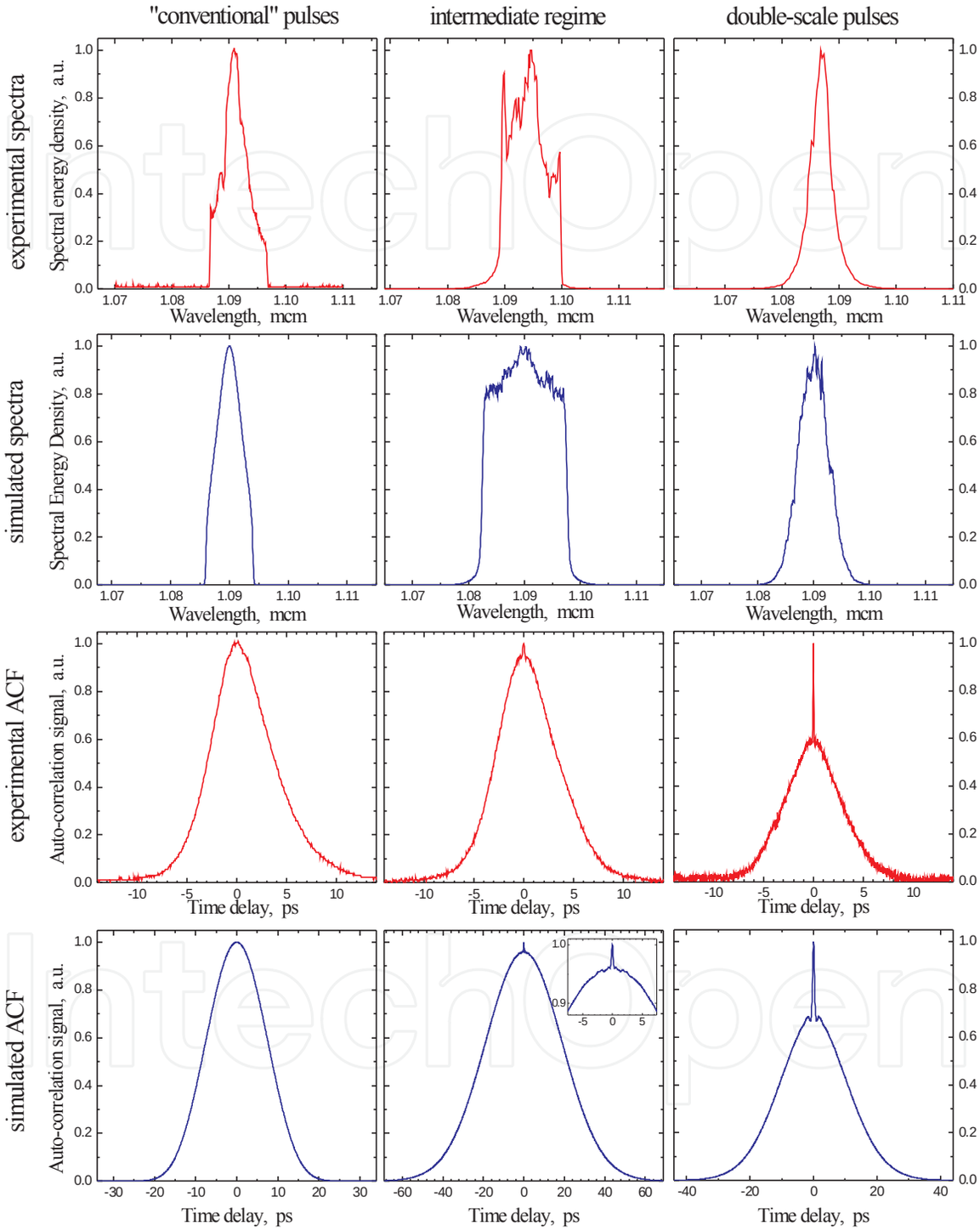

Figure 2. Experimentally measured (red) and simulated (blue) spectra and ACFs for three different lasing regimes: stable single-pulse (left column), intermediate (middle column) and noise-like generation (right column) [24].

http://dx.doi.org/10.5772/61956

where A_x and A_y are the polarisation components of the field envelope, z is the longitudinal coordinate along the fibre, t is the time in the retarded frame of reference, γ and β_2 are nonlinear and dispersion coefficients correspondingly, g_0 and P_{sat} stand for unsaturated gain coefficient and saturation power for the active fibre.

Equations (1, 2) describe propagation of radiation along an active fibre. Taking g_0=0, we can use the same equations to model laser pulse propagation inside passive resonator fibre. The fibre-optical polarisation beam splitter is represented in the model by the following matrix:

$$\hat{T}_{\text{PBS}} = \begin{pmatrix} 1 & 0 \\ 0 & 0 \end{pmatrix} \tag{3}$$

Unitary 2 × 2 matrices must be used to describe polarisation controllers. In particular, a polarisation controller based on the principle of fibre compression in the direction at an angle ϕ can be represented by a matrix introducing phase delay α rotated by angle ϕ by multiplying it by the corresponding rotation matrix:

$$\hat{T}_{\text{PC1}}(\alpha,\phi) = \begin{pmatrix} \cos\phi & -\sin\phi \\ \sin\phi & \cos\phi \end{pmatrix} \begin{pmatrix} e^{i\alpha/2} & 0 \\ 0 & e^{-i\alpha/2} \end{pmatrix} \begin{pmatrix} \cos\phi & \sin\phi \\ -\sin\phi & \cos\phi \end{pmatrix} \tag{4}$$

Parameter α in Eq. (4) stands for phase delay introduced by the polarisation controller and depends on the transverse fibre deformation. Similarly, a polarisation controller utilising fibre torsion can be expressed through its eigenvector projections: $\hat{T}_{\text{PC2}} = e^{i\alpha/2}\hat{P}_{+} + e^{-i\alpha/2}\hat{P}_{-}$, where circular polarisation state projections can be written as

$$\hat{P}_{\pm} = \frac{1}{2}\begin{pmatrix} 1 & \mp i \\ \pm i & 1 \end{pmatrix} \tag{5}$$

In order to model the propagation of laser pulses around the fibre cavity, Eqs. (1, 2) can be integrated numerically by the step-split Fourier method [26]. At the required points along the optical path, the polarisation transformations (3–5) are applied and losses corresponding to the intra-cavity elements are taken into account.

This modelling step is carried out repeatedly until a stationary state is reached. As a rule, anywhere between several hundred and several thousand modelled cavity round trips are needed, depending on the system parameters and the initial conditions, mostly taken as white noise or seed pulses. In certain cases, a laser may exhibit bistability: the limit cycle of the propagation equations may depend on the initial conditions. It is relevant to mention here that a similar phenomenon is observed in the experiment as hysteresis in switching between generation regimes [27]. If the limit cycle of the propagation equations corresponds to the 'conventional' pulse generation regime, the generation parameters (power, pulse duration,

spectrum width, *etc.*) of the limit cycle are highly stable (of the 10^{-3} order and higher). Conversely, when the laser generates double-scale pulses, the pulse parameters in the generated train fluctuate around their average values by a few per cent or even more between two successive cavity round trips. This circumstance can be used in modelling as a basic criterion to distinguish between generation regimes. We need to point out as well that the average generation parameters must be insensitive to variation within reasonable limits of the 'non-physical' modelling parameters, such as the mesh node count, mesh width and the step of numerical integration of Eqs. (1, 2). This has to be controlled during modelling.

The approach outlined in the foregoing paragraphs is sufficiently powerful and generalised to adequately model a variety of regimes observed in fibre lasers mode-locked due to NPE (see Fig. 2 and Ref. [24]), as well as NOLM/NALM and generation of both double-scale and 'regular' pulses. Such power and generality come, however, at the expense of very significant amount of computations necessary to perform in order to compare the model with the experiment. This downside results largely from the specific nature of fibre laser configurations relying on fibre-optical polarisation controllers. These controllers introduce a phase shift, which is impossible to directly measure in regular experimental implementations. As a consequence, for a valid match between modelling and experiment, it is necessary to perform a large series of computations for a range of settings of the intra-cavity polarisation controllers corresponding to a range of parameters α and ϕ in Eqs. (4, 5). For each set of parameters, the entire numerical modelling sequence has to be carried out, including specification of the initial conditions, multiple runs of radiation propagation along the cavity and analysis of the generation regime. In full analogy to the experiment, laser generation only emerges at certain combinations of intra-cavity polarisation element settings and levels of the pumping power launched into the active fibre. Therefore, a considerable part of calculations carried for randomly chosen polarisation controller parameters does not result in a pulsed generation regime. Nonetheless, this approach gives a fair idea of the great diversity of generation regimes accessible in an NPE-mode-locked fibre laser through adjustment of its settings. For instance, in Fig. 3, we present histograms of generation parameter distributions (rms bandwidth and rms pulse duration) for 'regular' and double-scale pulses generated in numerical modelling [7] at different settings of the polarisation controllers. Evidently, there is a considerable spread in laser parameter values, up to an order of magnitude and even wider. This result effectively indicates an opportunity to modify parameters of the output laser pulses (including double-scale ones) by adjusting the intra-cavity polarisation controllers in order to achieve optimal values for specific applications.

4. Simplified phenomenological model

Research in efficiency of double-scale pulses in practical applications ideally needs a less complicated numerical model, which would enable numerical studies at much more affordable expense of computation resources. With this objective, we have developed a phenomenological model of double-scale pulses relying on superposition of uncorrelated modes. Using this model, it is comparatively easy to re-create modelling pulses with parameters known from the

http://dx.doi.org/10.5772/61956

experiment (shape, duration and spectral width) for studying their various applications and parameter optimisation. The proposed phenomenological approach to modelling requires that the following function be calculated:

$$A(t) \sim \sqrt{P(t)} \cdot \sum_j A_j \exp\left(i\omega_j t\right). \tag{6}$$

Here, ω_j is the frequency of the j-th mode, t is the time, A_j is the complex amplitude of the j-th mode and $P(t)$ is the temporal pulse profile. The phases of complex amplitudes arg{ A_j } are taken as independent random values uniformly distributed over the range of 0–2π.

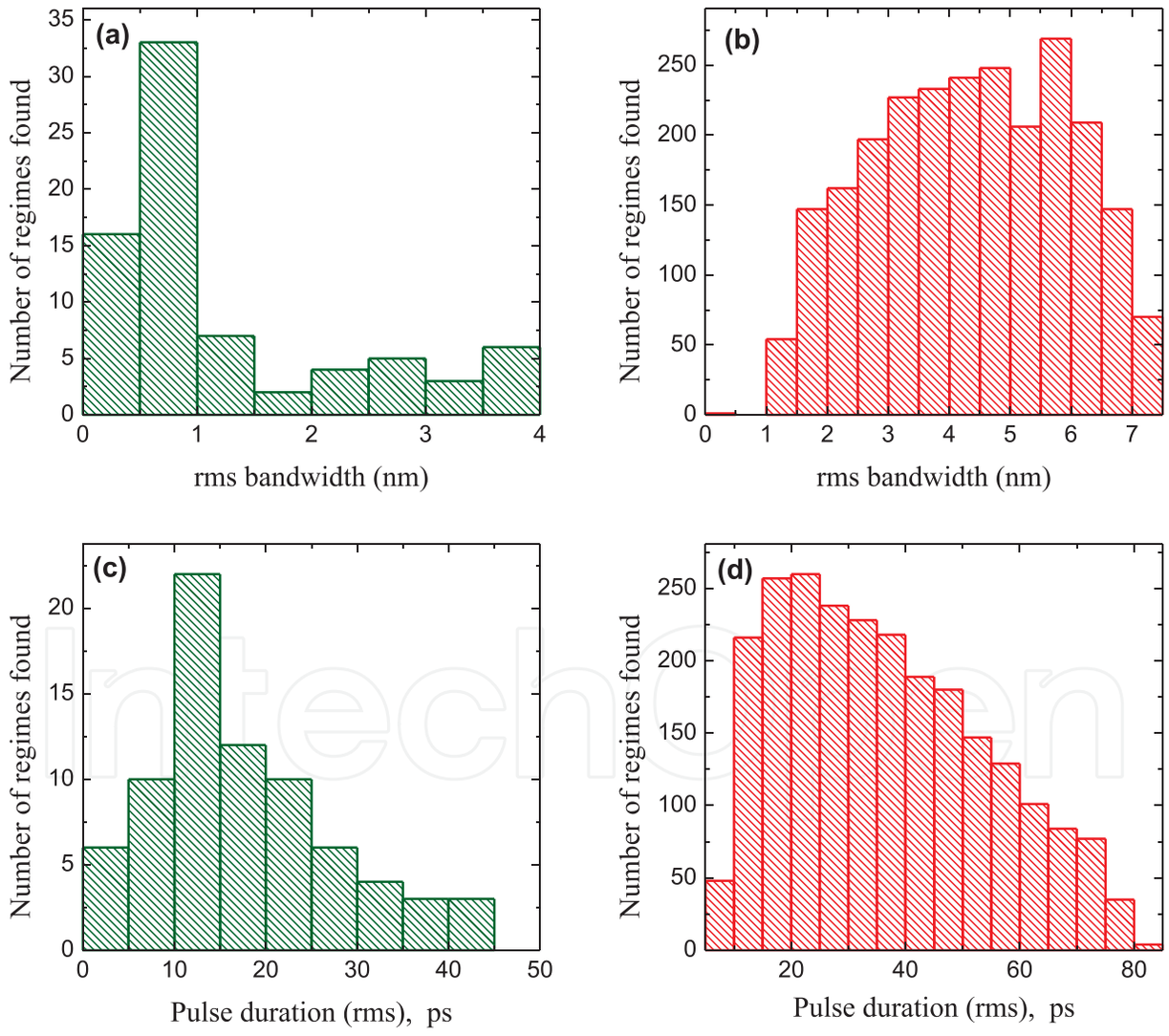

Figure 3. Rms bandwidth (a, b) and rms-pulse duration (c, d) variability in simulated 'conventional' (a, c) and double-scale (b, d) generation regimes [7].

In the simplest case, scalar values A_j in Eq. (6) can be assumed constant, while in more involved implementations of this model, their random character may also be taken into account ($|A_j|$ fluctuations). It is interesting to observe that the expression of Eq. (6) can be considered as a model of thermal (incoherent) source with a preset spectral profile. The sum part of Eq. (6) is multiplied by a specified profile $P(t)$, as a result shaping noise-like incoherent radiation into a pulse with a shape known from the experiment.

For an illustration, Fig. 4 presents the temporal distribution, spectrum and autocorrelation function of double-scale pulses generated in the simplified phenomenological model (Eq. (6)). It can be seen that the diagrams exhibit all the main features of double-scale pulses observed in both experiment and direct numerical modelling of laser generation (see Fig. 2). For instance, the temporal distribution of pulses in Fig. 4 looks like a wave packet stochastically filled with sub-pulses. Single-shot spectrum of the modelled pulses also has a noisy appearance, but the spectrum averaged over many pulses takes the form identical to that of $|A_j(\omega_j)|$ on condition that the duration of wave packets is much longer than the inverse spectrum width. The pulse ACF takes the shape of a broad pedestal with a narrow peak in its centre (Fig. 4 (c)). The relative pedestal magnitude is 0.5, and its width in the case of Gaussian pulses by a factor of $\sqrt{2}$ exceeds the duration of the pulse envelope $P(t)$ in Eq. (6)). The width of the central ACF peak, conversely, is equal to the inverse spectral width of pulses (see Fig. 4 (d)).

It should be noted here that although the proposed simplified model (Eq. (6)) is founded on the assumption of independent phases $arg\{A_j\}$ of modes (spectral radiation amplitudes), multiplication by $P(t)$ introduces correlation of neighbouring modes inside a spectral domain with the width of the order of pulse envelope $P(t)$ width. In reality, the level of an inter-mode correlation for double-scale pulses observed in the experiment and in direct numerical modelling may be higher than that of the explained simplified model. This is indicated by the ACF pedestal magnitude exceeding the 0.5 value in some generation regimes. In particular, the transient generation regime may be characterised by the maximum value of the central ACF peak much below unity (see Fig. 2). This corresponds to the strong inter-mode correlation and/or relatively small fluctuations.

The phenomenological model (Eq. (6)) analysed in the preceding discussion also improves our understanding of the origin of sub-pulses in the internal filling of double-scale pulses. According to Eq. (6), sub-pulses are closer in their nature to power oscillations resulting from interference of incoherent modes rather than to separate femtosecond pulses that are independent of each other. This circumstance leads to radical differences in behaviour of double-scale pulses undergoing temporal compression or stretching as compared with 'regular' laser pulses. This difference will be given a detailed treatment in the following section.

5. Pulse compression

One of the salient differences of double-scale pulses from 'conventional' laser pulses is related to limited possibilities of their compression. In most experimental configurations, double-scale

http://dx.doi.org/10.5772/61956

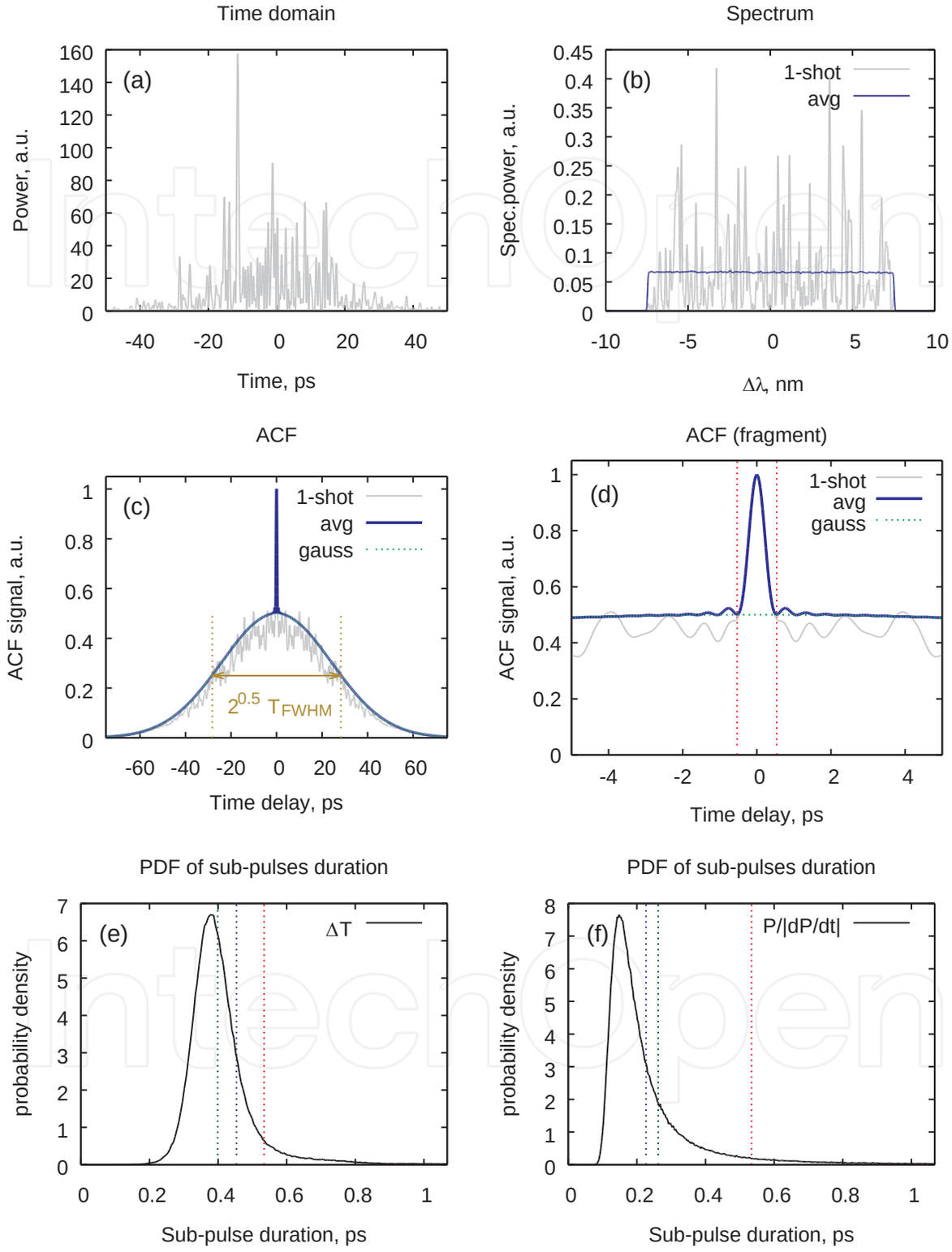

Figure 4. Time trace of power (a), spectral distribution (b) and ACF (c, d) of double-scale pulses in the simplified model. Red dotted line in (d) denotes the value of the inverse width of a Π-shaped spectrum. Grey lines correspond to single-shot traces and blue lines to those averaged over a large number of random realisations.

pulses are produced in fibre lasers with a significant positive dispersion of their cavities. If the laser generates 'conventional' pulses, the presence of uncompensated cavity dispersion leads to the formation of strongly chirped pulses. Such pulses can be subsequently compressed to a small fraction of their initial duration down to (or close to) the Fourier limit by passing them through optical compressors based on diffraction gratings, optical prisms and/or optical fibres with dispersion of different signs. Conversely, double-scale pulses present very limited possibilities of compression [24]. It has to be stressed that these limitations arise from the structure of the pulses themselves rather than from non-linear effects in fibre-optical compressors, which may also constrain compression coefficient of 'regular' laser pulses at sufficiently high-peak-power values [28].

Direct numerical modelling of laser generation based on coupled GNLSE (1, 2) explains the measured low compressibility of double-scale pulses in the experiment. As calculations demonstrated [24], unlike that of 'regular' pulses, the optical phase of double-scale pulses is not a smooth continuous function of time but rather is filled with fluctuations, as shown in Fig. 5. These phase fluctuations lead, in particular, to the lack of phase coherence across the seemingly regular array of pulses observed experimentally [29]. Fluctuations of the temporal dependence of the optical phase give rise to jitter of the instantaneous frequency of double-scale pulses. This, in turn, leads to presence at each moment in time (in each point within a double-scale pulse) of various frequencies covering the wide spectrum of the double-scale pulse, as can be readily seen in a simulated FROG diagram of Fig. 6. The fundamental principle of optical compression is to create a different temporal delay for the front and rear pulse edges, which have slightly different optical frequencies because of a pulse chirp. Passing along a phase-delay element, the components of the chirped pulse move closer to each other, producing the effect of pulse compression. Since different optical frequencies are present at each moment in double-scale pulses, frequency-dependent temporal delay of their components cannot compress such pulses as well as the 'regular' ones, as shown in Fig. 6.

Figure 6 showcases pulse spectrograms generated in direct numerical modelling of various generation regimes (indicated on top). The horizontal axis shows time in picoseconds and the vertical axis, frequency and wavelength λ (left- and right-hand axes, respectively). Radiation intensity is colour-coded on a log scale of 0 to –25 dB, as shown in the colour scale at the bottom of Fig. 6. Pulse duration in the included spectrograms corresponds to the horizontal dimension of intensity distribution, whereas the spectrum width corresponds to the vertical dimension. The distribution slant in the diagrams reflects the pulse chirp. Linear compressibility of pulses in optical compressors is predicated on the existence of chirp. The top row of diagrams demonstrates pulses exiting the laser and the bottom rows correspond to the result of various degrees of linear compression (the respective values of the optical compressor dispersion are specified to the left of the rows).

As seen in the left column of Fig. 6, the duration of 'regular' laser pulses may be reduced in a linear optical compressor almost down to the Fourier limit. The compression degree in this case is somewhat below the theoretical limit because of the non-linear chirp present at the pulse edges and clearly visible as pointed deformations of the colour patches of the left column in Fig. 6. In experiments, this limitation may be overcome by spectral filtration of such pulses:

http://dx.doi.org/10.5772/61956

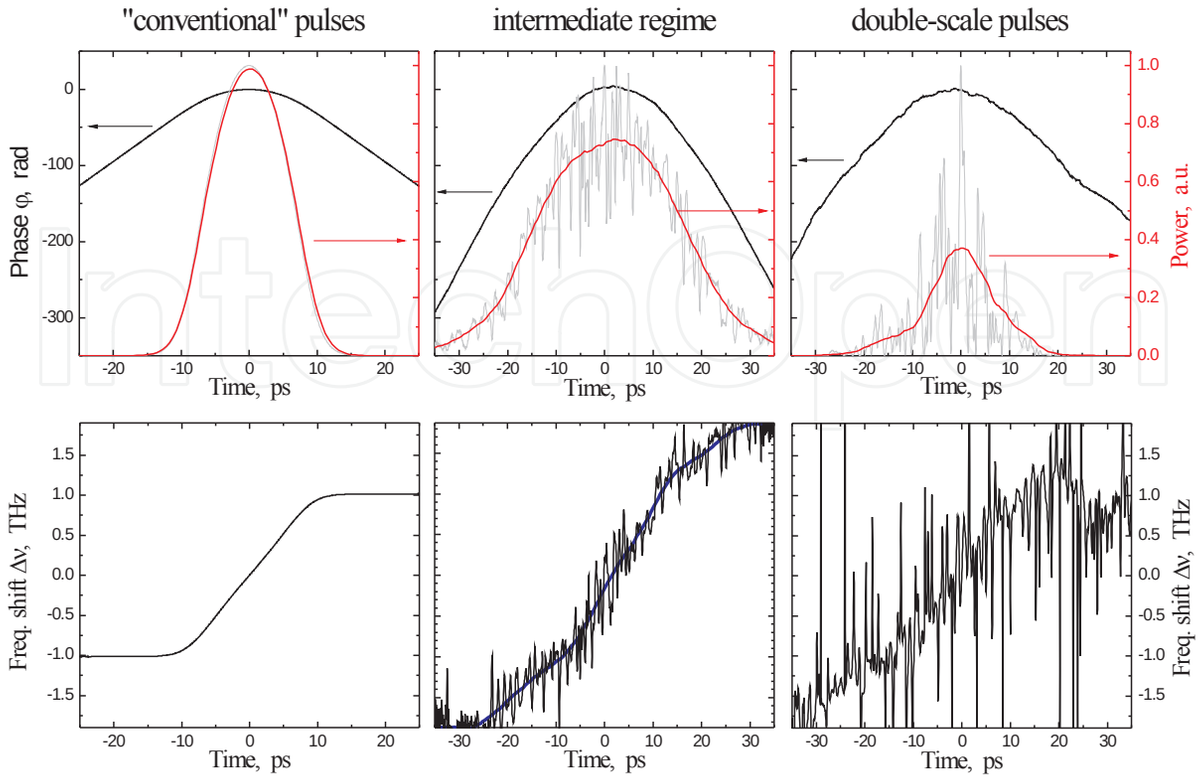

Figure 5. Simulated time dependencies of pulse power and phase (upper graphs), and frequency shifts (lower graphs) for different lasing regimes [24].

when the spectral extremities of chirped pulses are 'cut off', the temporal wings of these pulses containing non-linear chirps are also eliminated.

In contrast, double-scale pulses are not really amenable to compression (see the right column in Fig. 6). Although they have approximately three times the spectral width of a 'conventional' laser pulse (measured at –25 dB) in Fig. 6, after a pass through an optical compressor they retain a duration exceeding that of 'normal' pulses by a factor of over 5. Although these particular calculations indicate the possibility of almost twofold compression, the minimal achievable pulse duration far exceeds the Fourier limit, as a direct consequence of the pulse structure. At each moment in time (along any vertical section of the spectrogram), double-scale pulses contain practically all the components of its spectrum (see the bottom left diagram in Fig. 6).

The intermediate generation regime, with its comparatively low fluctuations of phase and other parameters of the generated pulses, takes an accordingly middle position with respect to linear compression, as indicated by the central column of Fig. 6. It is characterised by medium compressibility, which is limited by both factors mentioned earlier: the non-linear chirp (curved ends of the spectrogram) and phase fluctuations, making the spectrogram considerably wider than the spectrally limited pulses at the same or even at narrower spectrum width. This can be readily seen when comparing the central and left-hand diagrams in the bottom row of Fig. 6.

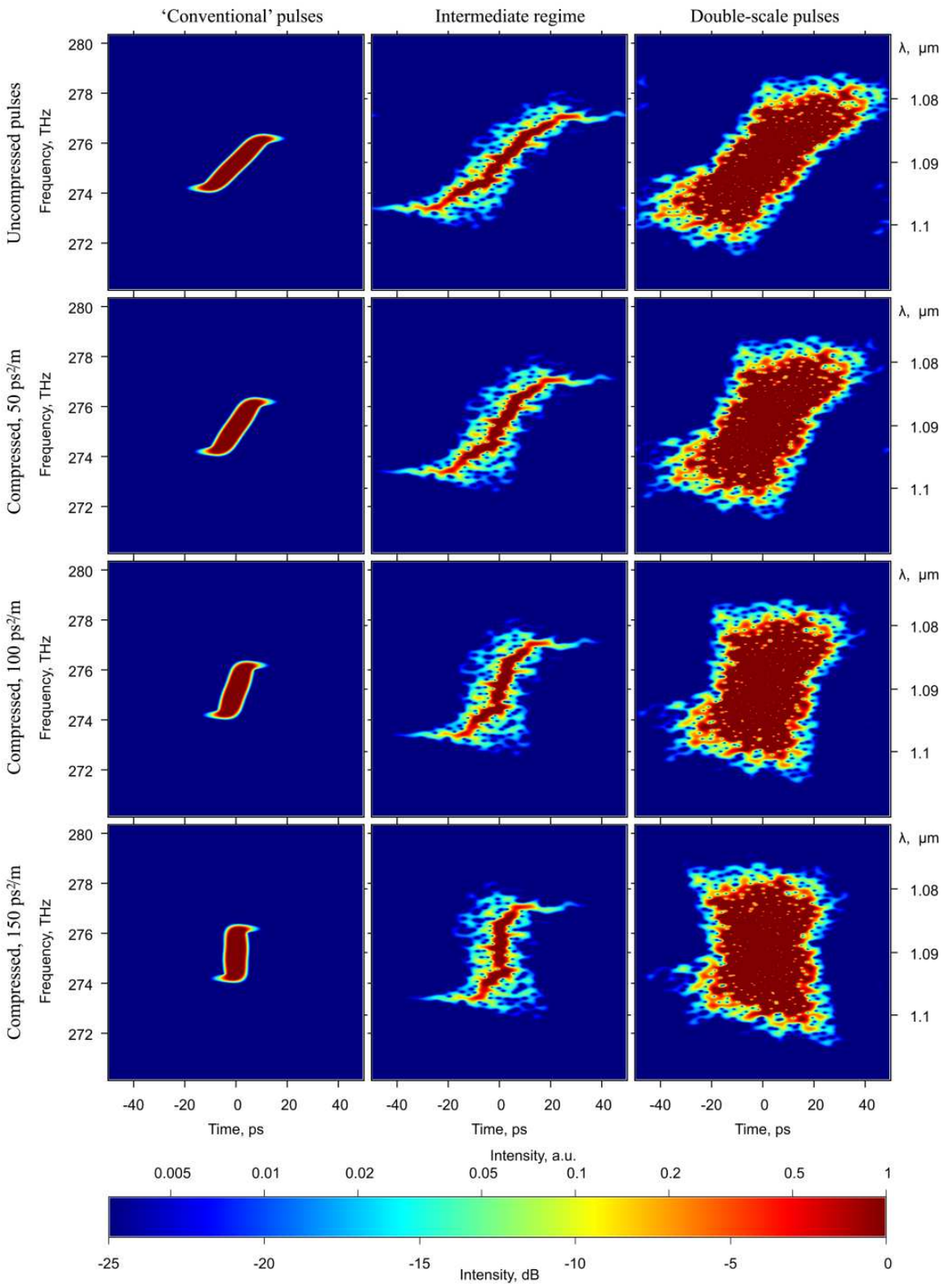

Figure 6. Simulated FROG of 'conventional' (left column), intermediate (at the middle) and double-scale (right column) pulses generated by all-normal-dispersion fibre laser passively mode-locked due to NPE and different stages of compression of these pulses.

http://dx.doi.org/10.5772/61956

6. Pulse stretching

It is clear that the optical phase fluctuations condition the difference of double-scale pulses from 'conventional' laser pulses not only in relation to compression but also to stretching, *i.e.*, to lengthening of the pulse duration as it propagates along a medium with chromatic dispersion (*e.g*. an optical fibre). Indeed, if we consider the diagrams of Fig. 6 in the reversed order (*i.e*. bottom to top instead of top to bottom, as before), we will observe dynamics of stretching of laser pulses with different levels of phase fluctuations in a dispersive medium. In this case, the bottom row of diagrams corresponds to the state with the smallest durations (for a given pulse type with a specific spectral width). Pulse duration increases during the process of propagation along the medium (see Fig. 6 from bottom to top).

The spectrograms presented in Fig. 6 demonstrate that double-scale pulses are significantly less stretchable than the 'regular' laser pulses of comparable or even narrower width of their optical spectrum. This circumstance makes double-scale pulses attractive in a number of applications where low temporal coherence of radiation is required, for example, to achieve high resolution in optical imaging. Unlike 'regular' ultrashort laser pulses with short coherence time, double-scale pulses may be delivered to the desired location over optical fibres practically without loss of the system's resolving power defined by the pulse coherence time.

7. Applications

Until recently, the possibility of practical application of double-scale pulses remained uncertain because stochastic filling of generated wave packets was understood to result in highly unstable output parameters. As it was experimentally shown, however, the average output power of a mode-locked fibre laser generating double-scale pulses remains relatively stable and pulse-to-pulse average power fluctuations being fairly small (a few per cent, as a rule). It was further discovered that double-scale pulses exhibit a number of remarkable properties making them radically different from 'usual' laser pulses. Double-scale pulses may carry relatively high energy (several μJ) directly at the output of a fibre master oscillator [21, 25]. Moreover, peak power of sub-pulses may far exceed the average peak power of the entire wave packet because of their short duration. It was also established that double-scale pulses feature comparatively high efficiency of non-linear interaction with the propagation medium in harmonic generation [8], Raman conversion [9] or super-continuum generation [10–13]. We analyse these and other promising applications of double-scale pulses in the following discussion.

The potential of double-scale pulses in configurations with non-linear frequency conversion is directly related to the high peak power of sub-pulse filling. The sub-pulse peak power may be several times as high as the average power of the double-scale envelope due to fluctuations resulting from stochastic nature of double-scale pulses. High peak power leads to relatively efficient non-linear optical transformation of double-scale pulses, for instance, harmonic generation, super-continuum generation, *etc*. As an illustration, let us consider the frequency-

doubling process in a thin non-linear crystal that we studied both in direct numerical modelling and in experiment [8]. Second-harmonic generation (SHG) was achieved in a Yb-doped fibre laser passively mode-locked due to NPE (see Fig. 1 for the optical layout). Through adjustment of the intra-cavity polarisation controllers, this laser could be switched between generation of 'regular' and double-scale pulses as needed during the experiment. Direct numerical modelling was carried out by integrating Eqs. (1, 2) with the following parameters: non-linear coefficient $\gamma = 4.7\times10^{-5}$ (cm•W)$^{-1}$, dispersion coefficient $\beta_2 = 23$ ps^2/km, small-signal gain $g_0 =$ 540 dB/km and saturation power of the active fibre $P_{sat} = 52$ mW.

Second-harmonic generation was further modelled with the following equation for the spectral wave amplitudes:

$$\frac{\partial A_{2n}}{\partial z} + \frac{1}{u}\frac{\partial A_{2n}}{\partial t} = -i\sigma_2 \sum_{j+k=n+1} A_{1j}A_{1k} \tag{7}$$

where A_{1j} and A_{2n} are spectral amplitudes of the first- and second-harmonic waves, respectively, u is the group velocity and σ_2 is the non-linear coefficient. Apart from the process of frequency doubling of the laser modes corresponding to terms with $j = k$, Eq. (7) also reflects processes of sum frequency generation (terms with $j \neq k$ under summation in Eq. (7)). Both types of processes are schematically shown in Fig. 7 (a) for $N = 3$ equidistantly spaced laser modes. Thick solid lines correspond to frequency doubling, and dotted lines show sum frequency generation. In reality, the number of laser modes N is very large; however, all of them are separated by the same distance $\Delta\omega$ from the neighbouring ones. The second-harmonic radiation, following Fig. 7 (a), will consist of $2N - 1$ equidistant modes spaced at the same spectral interval $\Delta\omega$.

Eq. (7) is integrable in the approximation of a thin non-linear crystal and in the absence of the pumping wave depletion. Assuming A_{1i} = constant along z and $A_{2n} = 0$ at $z = 0$, let us integrate Eq. (7) from 0 to L and divide the full power of the second-harmonic wave $I_{2n} = \Sigma|A_{2n}|^2$ by $(\sigma_2 L P_1)^2$, where P_1 is the first harmonic sum power:

$$\zeta = \left(\sum_n \left|\sum_{j+k=n+1} A_{1j}A_{1k}\right|^2\right) \cdot \left(\sum_j \left|A_{1j}\right|^2\right)^{-2} \tag{8}$$

The resulting coefficient ζ is the SHG relative efficiency, which equals to the ratio of two SH powers, of which the first is obtained when the non-linear crystal is pumped by a double-scale laser pulse with given mode amplitudes A_{1j} and the second is generated with the use of single-mode monochromatic pumping of the same power $P_1 = \Sigma|A_{1j}|^2$. An important feature of the dimensionless relative efficiency ζ is that it does not depend on power and thickness of the thin non-linear crystal but is sensitive to mode correlations and fluctuations, thus allowing us to easily compare different lasing regimes from the viewpoint of efficiency of non-linear frequency. To do that, we simulated the generation of double-scale pulses using Eqs. (1, 2) and

http://dx.doi.org/10.5772/61956

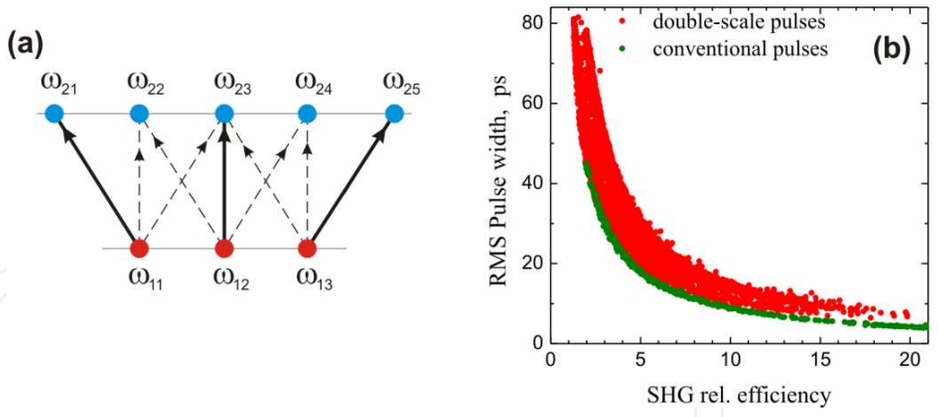

Figure 7. (a) Schematic diagram of SHG processes for $N = 3$ modes. (b) Correlation between relative SHG efficiency and rms pulse width of double-scale (red points) and conventional (green points) pulses.

averaged SHG relative efficiency (Eq. (8)) over multiple successive pulses produced by the fibre laser.

In our modelling, the parameters of the intra-cavity polarisation controllers were selected randomly. After 10,000 cavity passes, the generation mode of the modelled laser was analysed. If the laser generated double-scale or 'regular' pulses, then second-harmonic generation was modelled, which consisted in calculation of the relative efficiency ζ (Eq. (8)). Both the generation parameters and the ζ value were then saved by the program. The modelling cycle was then repeated with the intra-cavity polarisation controller settings chosen once again at random.

As a result of a large number of modelling cycles, statistical data were collected on the generation parameters and relative efficiency of frequency doubling in double-scale and 'regular' generation regimes. These data allowed the comparison of these regimes in relation to their efficiency for frequency doubling, and they also could be used to study the correlation between the frequency-doubling efficiency and the generation parameters. The most immediate link was identified between the relative efficiency of frequency doubling ζ and rms pulse duration T_{rms} with Pearson's correlation coefficient $\rho(\zeta, 1/T_{rms}) = 0.97$. The obtained results are presented in Fig. 7 (b). Each point on the shown diagram was generated as a result of direct numerical modelling of laser generation at fixed values of the intra-cavity polarisation controller settings. These values differ randomly between one point and another. The X-coordinates of the diagram points are proportional to the relative efficiency ζ of frequency doubling, whereas their Y-coordinates are proportional to the rms pulse width.

As it can be seen from Fig. 7 (b), ζ is roughly inversely proportional to T_{rms}, which means that ζ grows linearly with the pulse peak power, as it should for a second-order non-linear process. One can also note in Fig. 7 (b) that for any fixed pulse width T_{rms}, the relative SHG efficiencies are comparable for both regimes, being slightly higher for double-scale pulses. The experimental results that we measured in [8] agree with the numerical modelling, featuring higher efficiency of power transformation into the second harmonics for double-scale pulses in comparison to 'conventional' laser pulses.

We carried out similar experiments on cascaded Raman conversion of different pulse types in a long phosphosilicate fibre [9]. It was shown that feeding double-scale pulses into the fibre produces broader output spectrum as compared with using 'regular' laser pulses. Furthermore, different statistics of laser radiation in these regimes led to specific spectral features in the Raman spectrum of double-scale pulses [9]. In general, the results reported in Ref. [9] corroborate the conclusion made in the foregoing discussion about better efficiency of non-linear transformation of double-scale pulses.

Super-continuum generation [11, 30] may be also listed among promising applications related to non-linear frequency transformation. Apart from a relatively higher peak power, double-scale pulses are also less coherent. As it was demonstrated earlier, this may boost super-continuum generation and allow one to obtain wider and smoother supercontinuum spectra [11, 31, 32].

Two other prominent features of double-scale pulses, their very short coherence time and their broad spectrum [33–36], enable their application in imaging and sensor systems with high temporal and/or spatial resolution [37–39]. Importantly, double-scale pulses are not strongly affected by dispersive broadening [1], unlike regular ultrashort laser pulses with comparable coherence time. This makes it possible to transmit such pulses over optical fibres towards the target objects without loss of system's resolving power.

Inner structure of double-scale pulses filled with ultrashort sub-pulses and their significant spectrum width also make them attractive for applications such as laser-induced breakdown spectroscopy (LIBS) [6], a type of atomic emission spectroscopy. High-energy laser pulses are focused on a surface and cause ablation and plasma formation. The radiation generated by plasma is then registered in an optical system for spectral analysis. Comparison of recorded spectral lines with the known atomic optical spectra allows relatively easy and fast identification of the chemical composition of the studied sample. This method has the advantages of needing little or no sample preparation, and the possibility of depth profile generation by layer-wise ablation of material from the sample surface. This latter circumstance also solves the problem of surface contamination of the studied samples. Another important benefit of LIBS is its minimally or non-destructive nature. LIBS features sufficiently high precision and does not rely on ionising radiation, which is important for biological safety. Double-scale pulses generated in passively mode-locked fibre lasers present a virtually ideal solution for LIBS, because they deliver bursts of femtosecond sub-pulses at megahertz repetition rates [6]. High peak power of their sub-pulses drives correspondingly high efficiency of two-photon processes while maintaining low thermal stress of the studied samples.

8. Conclusions

Double-scale pulses offer a number of unique properties, including comparatively high peak power, broad spectral width and low coherence time. Therefore, such pulses hold much promise in a number of applications (*e.g.* non-linear optical frequency transformation, spectroscopy, material micro-processing and imaging techniques). They furthermore exhibit

a wide variety of generation regimes and an improbable combination of stochastic and coherent laser dynamics, still far from being understood. Although this factor draws the attention of researchers to double-scale pulses, it also prevents, for the time being, broader applications of double-scale pulses in research and technology applications of fibre lasers.

Acknowledgements

This work was supported by the Grants of Ministry of Education and Science of the Russian Federation (agreement No. 14.B25.31.0003, ZN-06-14/2419, order No. 3.162.2014/K).

Author details

Sergey Kobtsev*, Sergey Smirnov and Sergey Kukarin

*Address all correspondence to: sergey.kobtsev@gmail.com

Division of Laser Physics and Innovative Technologies, Novosibirsk National Research State University, Novosibirsk, Russia

References

[1] M. Horowitz, Y. Barad, and Y. Silberberg, "Noiselike pulses with a broadband spectrum generated from an erbium-doped fiber laser," Opt. Lett. 22(11), 799–801 (1997).

[2] O. Pottiez, R. Grajales-Coutiño, B. Ibarra-Escamilla, E. A. Kuzin, and J. C. Hernández-García, "Adjustable noiselike pulses from a figure-eight fiber laser," Appl. Opt. 50(25), E24–E31 (2011).

[3] D. Lei, H. Yang, H. Dong, S. Wen, H. Xu, and J. Zhang, "Effect of birefringence on the bandwidth of noise-like pulse in an erbium-doped fiber laser," J. Mod. Opt. 56(4), 572–576 (2009).

[4] Rare-Earth-Doped Fiber Lasers and Amplifiers, Revised and Expanded. Ed. M. J. Digonnet. CRC Press, New York, 2001. M. E. Fermann, and Martin Hofer, Chapter 8 "Mode-locked fiber lasers", pp. 499-500.

[5] S. Kobtsev, S. Kukarin, S. Smirnov, S. Turitsyn, and A. Latkin, "Generation of double-scale femto/pico-second optical lumps in mode-locked fiber lasers," Opt. Express 17, 20707–20713 (2009).

[6] B. Nie, G. Parker, V. V. Lozovoy, and M. Dantus, "Energy scaling of Yb fiber oscillator producing clusters of femtosecond pulses," Opt. Eng. 53(5), 051505 (2014).

[7] S. Kobtsev, S. Smirnov, S. Kukarin, and S. Turitsyn, "Mode-locked fiber lasers with significant variability of generation regimes," Opt. Fiber Technol. 20(6), 615–620 (2014).

[8] S. Smirnov, S. Kobtsev, and S. Kukarin, "Efficiency of non-linear frequency conversion of double-scale pico-femtosecond pulses of passively mode-locked fiber laser," Opt. Express 22(1), 1058–1064 (2014).

[9] S. Kobtsev, S. Kukarin, S. Smirnov, and I. Ankudinov, "Cascaded SRS of single- and double-scale fiber laser pulses in long extra-cavity fiber," Opt. Express 22(17), 20770–20775 (2014).

[10] S. M. Kobtsev, S. V. Kukarin, and S. V. Smirnov, "All-fiber high-energy supercontinuum pulse generator," Laser Phys. 20(2), 375–378 (2010).

[11] J. C. Hernandez-Garcia, O. Pottiez, and J. M. Estudillo-Ayala, "Supercontinuum generation in a standard fiber pumped by noise-like pulses from a figure-eight fiber laser," Laser Phys. 22(1), 221–226 (2012).

[12] A. Zaytsev, C. H. Lin, Y. J. You, C. C. Chung, C. L. Wang, and C. L. Pan, "Supercontinuum generation by noise-like pulses transmitted through normally dispersive standard single-mode fibers," Opt. Express 21(13), 16056–16062 (2013).

[13] S. S. Lin, S. K. Hwang, and J. M. Liu, "Supercontinuum generation in highly nonlinear fibers using amplified noise-like optical pulses," Opt. Express 22(4), 4152–4160 (2014).

[14] D. V. Churkin, S. Sugavanam, N. Tarasov, S. Khorev, S. V. Smirnov, S. M. Kobtsev, and S. K. Turitsyn, "Stochasticity, periodicity and localized light structures in partially mode-locked fibre lasers," Nat. Commun. 6, 7004, 1–6 (2015). doi:10.1038/ncomms8004

[15] Q. Wang, T. Chen, M. Li, B. Zhang, and Y. Lu, "All-fiber ultrafast thulium-doped fiber ring laser with dissipative soliton and noise-like output in normal dispersion by single-wall carbon nanotubes," Appl. Phys. Lett. 103, 011103-1–3 (2013).

[16] Y. Chen, M. Wu, P. Tang, S. Chen, J. Du, G. Jiang, Y. Li, C. Zhao, H. Zhang, and S. Wen, "The formation of various multi-soliton patterns and noise-like pulse in a fiber laser passively mode-locked by a topological insulator based saturable absorber," Laser Phys. Lett. 11(5), 055101 (2014).

[17] Y. S. Fedotov, A. V. Ivanenko, S. M. Kobtsev, and S. V. Smirnov, "High average power mode-locked figure-eight Yb fibre master oscillator," Opt. Express 22(25), 31379–31386 (2014).

[18] O. Pottiez, R. Grajales-Coutiño, B. Ibarra-Escamilla, E. A. Kuzin, and J. C. Hernández-García, "Adjustable noiselike pulses from a figure-eight fiber laser," Appl. Opt. 50 (25), E24–E31 (2011).

[19] S. M. Kobtsev and S. V. Smirnov, "Fiber lasers mode-locked due to nonlinear polarization evolution: golden mean of cavity length," Laser Phys., 21(2), 272–276 (2011).

[20] I. A. Yarutkina, O. V. Shtyrina, M. P. Fedoruk, and S. K. Turitsyn, "Numerical modeling of fiber lasers with long and ultra-long ring cavity," Opt. Express 21(10), 12942–12950 (2013).

[21] S. Kobtsev, S. Kukarin, and Yu. Fedotov, "Ultra-low repetition rate mode-locked fiber laser with high-energy pulses," Opt. Express 16(26), 21936–21941 (2008).

[22] P. Grelu and N. Akhmediev, "Dissipative solitons for mode-locked lasers," Nat. Photonics 26, 84–92 (2012).

[23] L. Wang, X. Liu, Y. Gong, D. Mao, and L. Duan, "Observations of four types of pulses in a fiber laser with large net-normal dispersion," Opt. Express 19, 7616–7624 (2011).

[24] S. Smirnov, S. Kobtsev, S. Kukarin, and A. Ivanenko, "Three key regimes of single pulse generation per round trip of all-normal-dispersion fiber lasers mode-locked with nonlinear polarization rotation," Opt. Express 20(24), 27447–27453 (2012).

[25] S.V.Smirnov, S.M. Kobtsev, S.V.Kukarin and S.K.Turitsyn (2011). Mode-locked fibre lasers with high-energy pulses, Laser systems for applications, Dr Krzysztof Jakubczak (Ed.), ISBN: 978-953-307-429-0, InTech, DOI: 10.5772/24360. Available from: http://www.intechopen.com/books/laser-systems-for-applications/mode-locked-fibre-lasers-with-high-energy-pulses.

[26] G. P. Agrawal, Nonlinear Fiber Optics, third ed., Academic Press, San Diego, USA 2001.

[27] A. Komarov, H. Leblond, and F. Sanchez, "Multistability and hysteresis phenomena in passively mode-locked fiber lasers," Phys. Rev. A 71, 053809-1–9 (2005).

[28] S. V. Smirnov, S. M. Kobtsev, and S. V Kukarin. "Linear compression of chirped pulses in optical fibre with large step-index mode area," Opt. Express 23(4), 3914–3919 (2015).

[29] A. F. J. Runge, C. Aguergaray, N. G. R. Broderick, and M. Erkintalo, "Coherence and shot-to-shot spectral fluctuations in noise-like ultrafast fiber lasers," Opt. Letters 38 (21), 4327–4330 (2013).

[30] L. Wang, X. Liu, Y. Gong, D. Mao, and L. Duan, "Observations of four types of pulses in a fiber laser with large net-normal dispersion," Opt. Express 19 (8), 7616–7624 (2011).

[31] F. Vanholsbeeck, S. Martin-Lopez, M. González-Herráez, and S. Coen, "The role of pump incoherence in continuous-wave supercontinuum generation," Opt. Express 13 (17), 6615–6625 (2005).

[32] S. Kobtsev and S. Smirnov, "Modelling of high-power supercontinuum generation in highly nonlinear, dispersion shifted fibers at CW pump," Opt. Express 13 (18), 6912–6918 (2005).

[33] Y. Takushima, K. Yasunaka, Y. Ozeki, and K. Kikuchi, "87 nm bandwidth noise-like pulse generation from erbium-doped fibre laser," Electron. Letters 41, 399–400 (2005).

[34] L. M. Zhao, D. Y. Tang, T. H. Cheng, H. Y. Tam, and C. Lu, "120 nm bandwidth noise-like pulse generation in an erbium-doped fiber laser," Opt. Commun. 281, 157–161 (2008).

[35] L. A. Vázquez-Zuñiga and Y. Jeong, "Super-broadband noise-like pulse erbium-doped fiber ring laser with a highly nonlinear fiber for Raman gain enhancement," IEEE Photonic. Technol. Lett. 24, 1549–1551 (2012).

[36] L. A. Vazquez-Zuniga and Y. Jeong, "Super-broadband noise-like pulse Erbium-doped fiber ring laser with a highly nonlinear fiber for Raman gain enhancement," IEEE Photonic. Technol. Lett. 24 (17), 1549–1551 (2012).

[37] S. Keren, A. Rosenthal, and M. Horowitz. "Measuring the structure of highly reflecting fiber Bragg gratings," IEEE Photonic. Technol. Lett. 15(4), 575–577 (2003).

[38] V. Goloborodko, S. Keren, A. Rosenthal, B. Levit, and M. Horowitz, "Measuring temperature profiles in high-power optical fiber components," Appl. Opt. 42(13), 2284–2288 (2003).

[39] S. Keren and M. Horowitz, "Interrogation of fiber gratings by use of low-coherence spectral interferometry of noiselike pulses," Opt. Lett. 26(6), 328–330 (2001).